

NASA Technical Memorandum 81347

**FRICION CHARACTERISTICS OF STEEL SKIDS EQUIPPED
WITH SKEGS ON A LAKEBED SURFACE**

Walter J. Sefic

December 1979



NASA Technical Memorandum 81347

**FRICITION CHARACTERISTICS OF STEEL SKIDS EQUIPPED
WITH SKEGS ON A LAKEBED SURFACE**

Walter J. Sefic

**Dryden Flight Research Center
Edwards, California**



**National Aeronautics and
Space Administration**

1979

FRICION CHARACTERISTICS OF STEEL SKIDS EQUIPPED WITH SKEGS ON A LAKEBED SURFACE

Walter J. Sefic
Dryden Flight Research Center

INTRODUCTION

Skid type landing gears have been used on a number of flight vehicles, including the X-2 and X-15 aircraft and the F-15 remotely piloted research vehicles (RPRV). Some advantages of skid type landing gears are reliability, the ability to withstand aerodynamic heating, minimization of landing space requirements, and ability to sustain high landing speeds.

The friction characteristics of skids made of various materials have been studied. The results of experimental ground tow tests are given in reference 1. Data for various skid materials on dissimilar lakebed surfaces are presented in reference 2. The F-15 RPRV (refs. 3 and 4) utilized skids on the main gear and the nose gear. To improve directional stability during landing, small protruding runners or skegs were added to the bottom of the main F-15 RPRV landing gear skids. The success of this system led to a decision to utilize the same technique for the highly maneuverable aircraft technology (HiMAT) vehicle, which is also an RPRV and is intended for lakebed landings. The first tests of the HiMAT landing gear system on a test vehicle (fig. 1) indicated that the coefficients of friction were higher than expected. Therefore, tests were made to determine the coefficient of friction for skids with skegs on a lakebed surface. Eight tests were made with various skleg configurations. This paper presents the results of the investigation.

TEST DESCRIPTION

Test Vehicle

The test vehicle (fig. 1) consisted of a structural steel framework which simulated the dimensional and mass characteristics of the HiMAT vehicle. The main gear was simulated by using square structural tubing that was instrumented to measure vertical and drag loads (fig. 2). The test vehicle was attached to a tractor-trailer combination by means of a pinned connection at the front, and it was suspended at the center of gravity by .48 centimeter cable. The distance between the bottom of the skid and the lakebed prior to drop was approximately 5.0 centimeters.

Test Procedure

The procedure consisted of stabilizing the tractor-trailer test vehicle combination at maximum speed (approximately 22.3 m/sec) and cutting the suspension cable with a pyrotechnic cable cutter. The test vehicle then rotated about the front pinned connection and struck the lakebed surface. The truck operator then allowed the vehicle to coast in gear until its speed decreased to approximately 9 meters per second, at which point the driver applied brakes to bring the vehicle to a stop. Typical slideout distance for all tests was approximately 500 meters. Typical slideout tracks on the lakebed are shown in figure 3.

The four configurations indicated in figure 4 were tested. The skids were constructed of 4130 steel. Each configuration was tested twice, for a total of eight test conditions. The second test on each configuration was performed in a slightly different lakebed location.

INSTRUMENTATION AND CALIBRATION

The simulated right hand main gear was instrumented with strain gage bridges to measure vertical and drag loads (figs. 2 and 5). The outputs of strain gage bridges A and B were combined in equations to measure vertical load and drag load. The output of strain gage bridge C was utilized in an equation to measure drag load only. The calibration was performed in the Dryden Flight Research Center Loads Facility (ref. 5) and consisted of applying three load conditions to the gear in a calibration rig (fig. 6). The loads were applied in 20 percent increments from zero to maximum load and back to zero as indicated in table 1. Typical strain gage bridge outputs are shown in figure 7 for the combined vertical and drag calibration load.

TABLE 1. CALIBRATION LOAD CONDITIONS

Load condition	Maximum vertical load, newtons	Maximum drag load, newtons
1	44,482	0
2	0	22,241
3	44,482	22,241

Load equations were developed for the vertical and drag load from strain gage bridges A and B utilizing least square multiple regressions of load conditions 1, 2, and 3, based on a technique described in reference 6.

An equation for drag load was also obtained from a least square slope of load versus strain gage output from bridge C for load condition 2.

Data for the calibration and the lakebed tests were recorded on a 9-bit pulse code modulation (PCM) telemetry system at 200 samples per channel per second. A ground-based computer was used to analyze the data.

Accuracy

The accuracy of the loads measurements and the resulting friction coefficients were obtained from the standard error (σ) of the regression equations (ref. 6) and from the progressive error technique described in reference 7. The resulting estimates of accuracy are given in table 2.

TABLE 2. ACCURACIES

Parameter	Description	Accuracy
$Vert_{AB}$	Vertical load measured with strain gages A and B	± 463 N
$Drag_{AB}$	Drag load measured with strain gages A and B	± 476 N
$Drag_C$	Drag load measured with strain gage C	± 58 N
F_{AB}	Friction coefficient $F_{AB} = \frac{Drag_{AB}}{Vert_{AB}}$	$\pm .05$
F_C	Friction coefficient $F_C = \frac{Drag_C}{Vert_{AB}}$	$\pm .03$
F_{AV}	Friction coefficient $F_{AV} = \frac{F_{AB} + F_C}{2}$	$\pm .04$

An additional check on accuracy was determined by substituting the data from load condition 3 (table 1) and the combined vertical and drag load into the loads equations and plotting the resulting data as function of applied load (figs. 8 and 9). The data in figures 8 and 9 agree with the accuracies listed in table 2.

DISCUSSION OF RESULTS

The friction coefficient values were obtained from data recorded after the test rig had stabilized, within 3 seconds after impact. Each friction coefficient data point was obtained by averaging 200 samples of data. Since the data acquisition system sampled at 200 samples per channel per second, each data point represents 1 second of data. The data in table 3 indicate an increase in the friction coefficient of approximately 47 percent due to the installation of a 1.27 centimeter skeg to the bottom of the skid. A skeg with a depth of only .64 centimeter resulted in an increase of approximately 16 percent over the flat skid. As indicated in table 3, each test was run twice. The second run was conducted on a different area of the lakebed than the first.

Time histories of the eight tests are shown in figure 10. As in table 3, each data point in figure 10 represents the average of 200 data points. Data from reference 2 are indicated in the time histories by a solid line for comparison purposes. The data from reference 2 are for 4130 flat steel skids taken at a speed of 22 meters per second. As figure 10 shows, the data in reference 2 agree favorably with the data for the skid tested with no skeg.

As indicated in table 2 and figure 10, the addition of a 30° bevel to the leading edge of the skeg had little or no effect on the magnitude of the friction coefficient.

TABLE 3. FRICTION COEFFICIENTS

Test number	Friction coefficient			Skeg configuration
	F _{AB}	F _C	F _{AV}	
1	.54	.53	.53	Full skeg
2	.54	.53	.53	Full skeg
3	.53	.50	.52	Full skeg with 30° bevel
4	.57	.54	.55	Full skeg with 30° bevel
5	.51	.48	.50	1/2 skeg with 30° bevel
6	.41	.42	.41	1/2 skeg with 30° bevel
7	.37	.38	.37	No skeg
8	.37	.35	.36	No skeg

CONCLUDING REMARKS

Friction characteristics were obtained from tests conducted on 4130 steel skids with and without skegs.

The addition of a 1.27 centimeter deep skeg to the bottom of the skeg caused the coefficient of friction to increase from an average value of .36 to .53, a 47 percent increase in friction coefficient compared with the flat bottomed skid.

The addition of a .64 centimeter deep skeg to the bottom of the skeg caused the coefficient of friction to increase from .36 to .46, a 16 percent increase in friction coefficient compared with the flat skid.

The modification of the skeg by beveling the leading edge had little or no effect on the magnitude of the friction coefficient.

Data from another study of the same type of steel skids without skegs agreed favorably with the data of this report for skids without skegs at a speed of 22 meters per second.

REFERENCES

1. Dreher, Robert C.; and Batterson, Sidney A.: Coefficients of Friction and Wear Characteristics for Skids Made of Various Metals on Concrete, Asphalt, and Lakebed Surfaces. NASA TN D-999, 1962.
2. Wilson, Ronald J.: Drag and Wear Characteristics of Various Skid Materials on Dissimilar Lakebed Surfaces During the Slideout of the X-15 Airplane. NASA TN D-3331, 1966.
3. Layton, G. P.: NASA Flight Research Center Scale F-15 Remotely Piloted Research Vehicle Program. Advancements in Flight Test Engineering, Soc. Flight Test Eng., Aug. 1974, pp. 1-63--1-76.
4. Lockenour, Jerry L.; and Layton, Garrison P.: RPRV Research Focus on HiMAT. Astronaut. & Aeronaut., Apr. 1976, pp. 36-41.
5. Sefic, Walter J.; and Anderson, Karl F.: NASA High Temperature Loads Calibration Laboratory. NASA TM X-1868, 1969.
6. Skopinski, T. H.; Aiken, William S., Jr.; and Huston, Wilber B.: Calibration of Strain-Gage Installations in Aircraft Structures for the Measurement of Flight Loads. NACA Rept. 1178, 1954.
7. McCracken, Daniel D.; and Dorn, William S.: Numerical Methods and Fortran Programming. John Wiley & Sons, Inc., 1964.

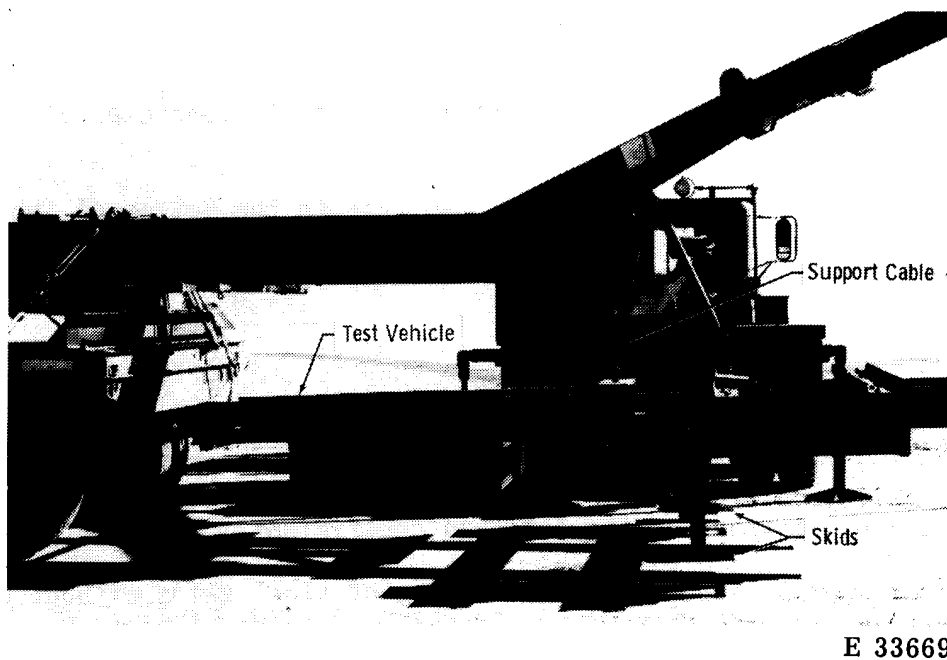


Figure 1. Test vehicle utilized for friction coefficient determination.

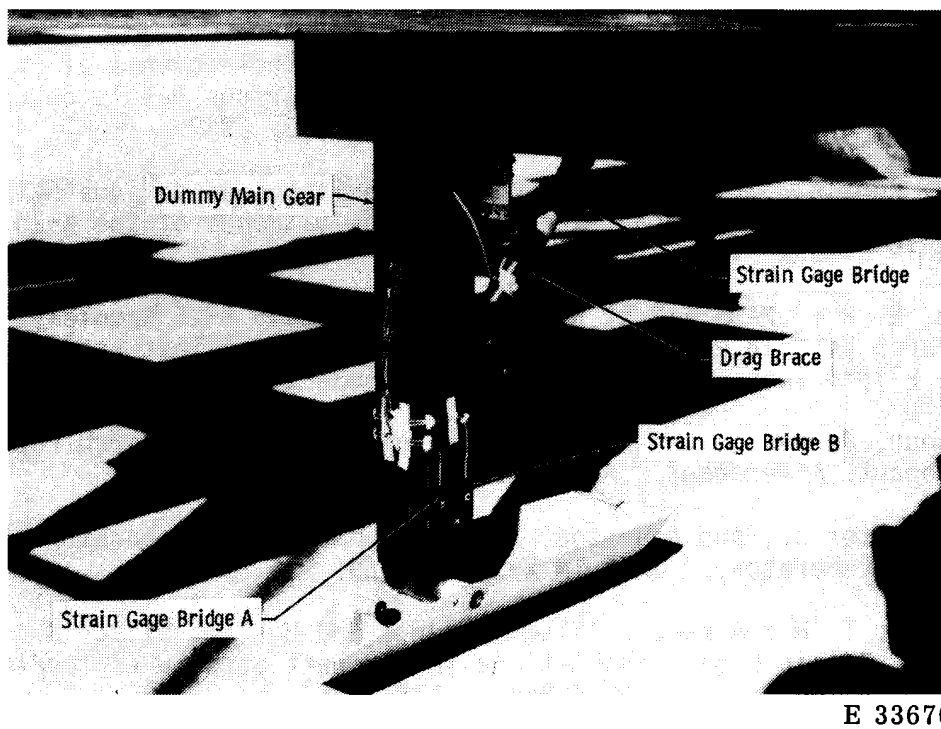
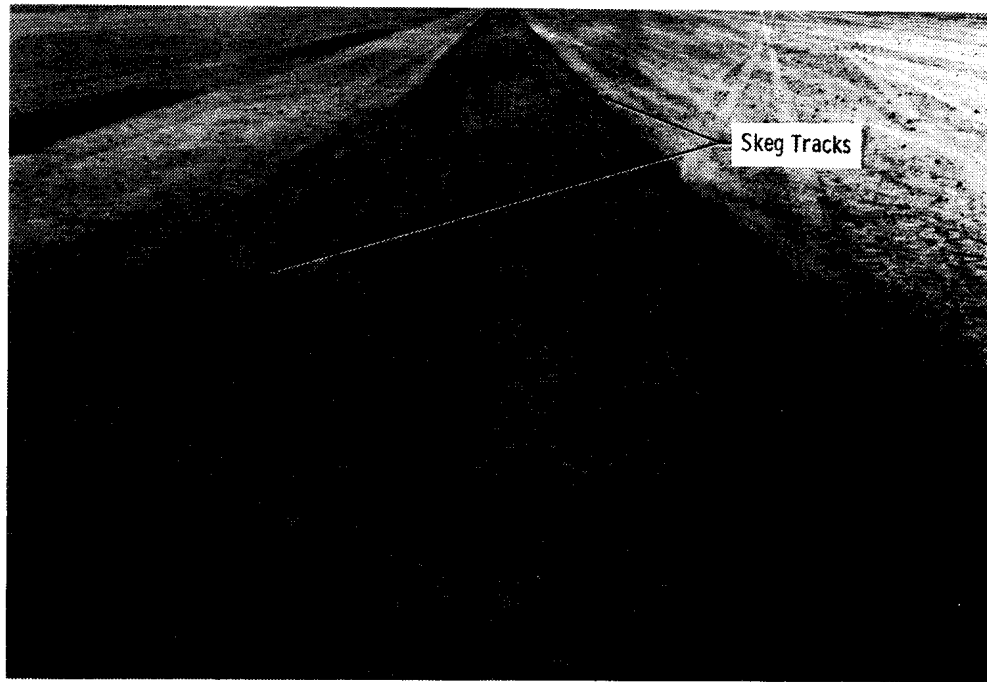


Figure 2. Strain gage locations on dummy main landing gear.



E 33672

Figure 3. Typical slideout tracks for skid with skeg configuration.

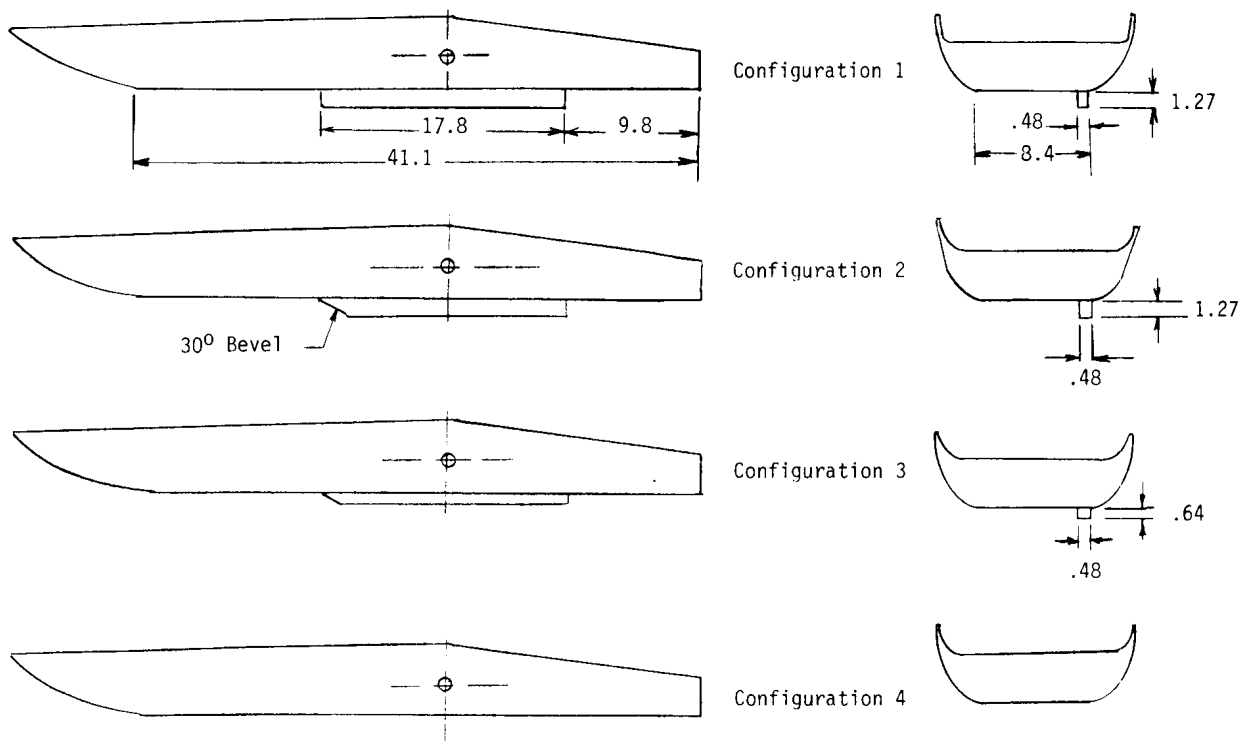
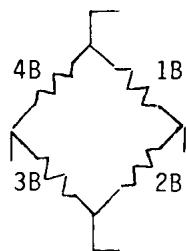


Figure 4. Skid configurations used in friction coefficient tests. All dimensions in centimeters.

Typical bridge circuit for
bridges A, B, and C



Gages 2B and 4B
mounted on opposite
face

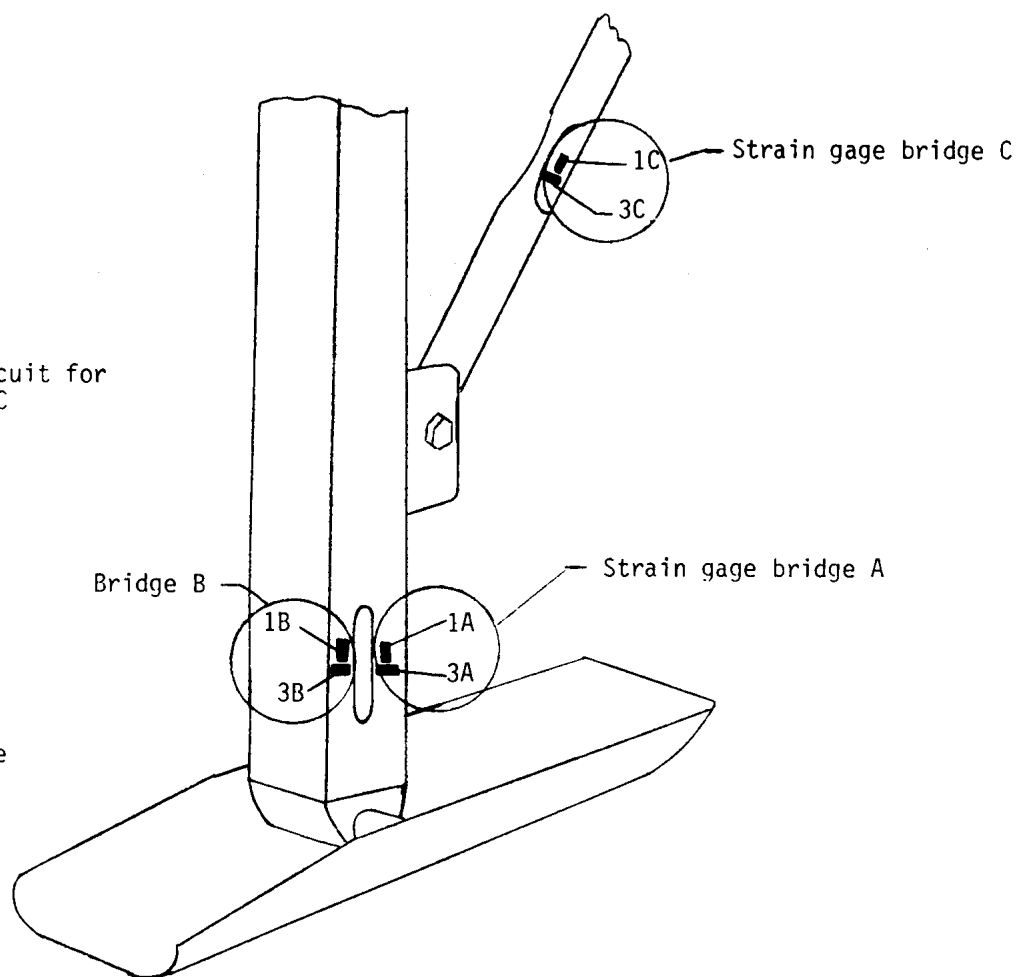


Figure 5. Strain gage locations on simulated HiMAT main landing gear to measure vertical and drag loads.

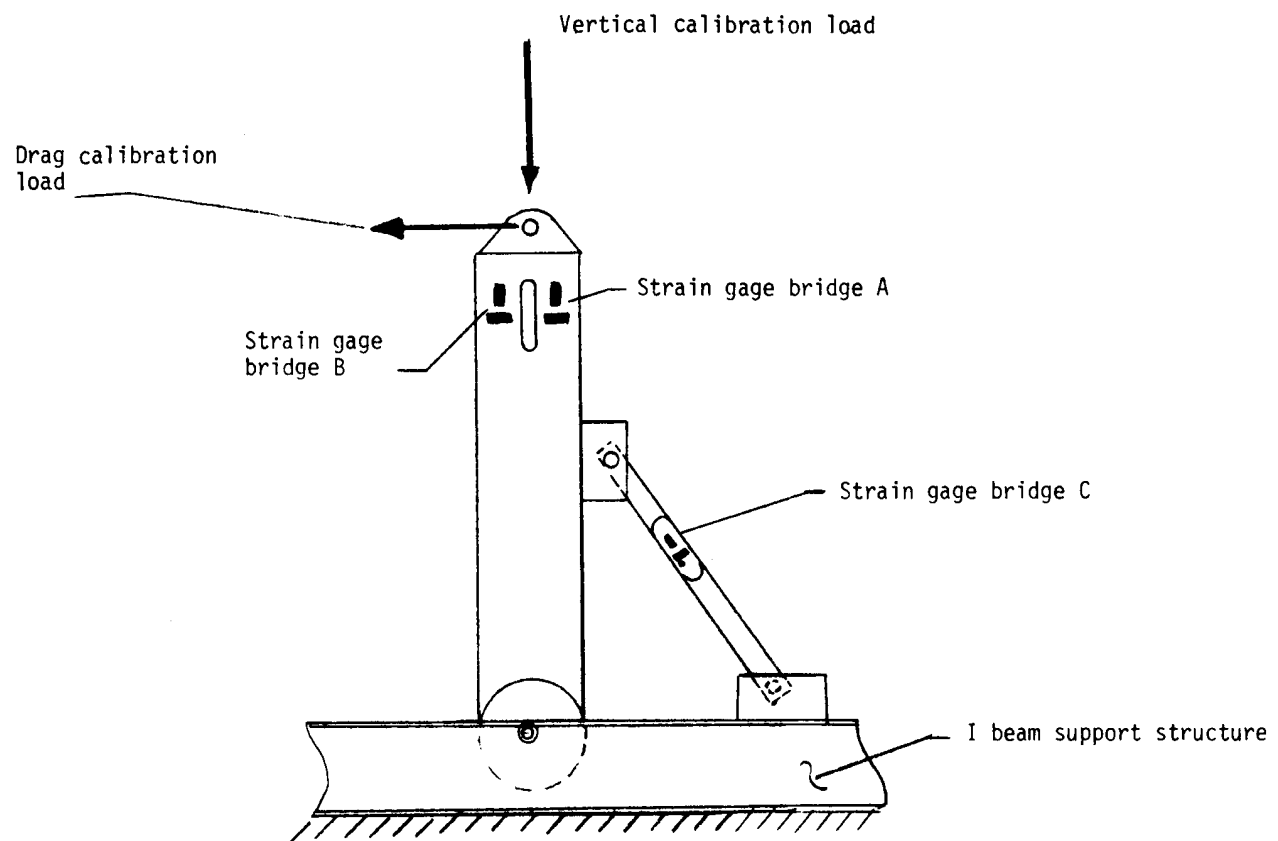


Figure 6. Rig utilized for applying calibration loads to a simulated HiMAT landing gear.

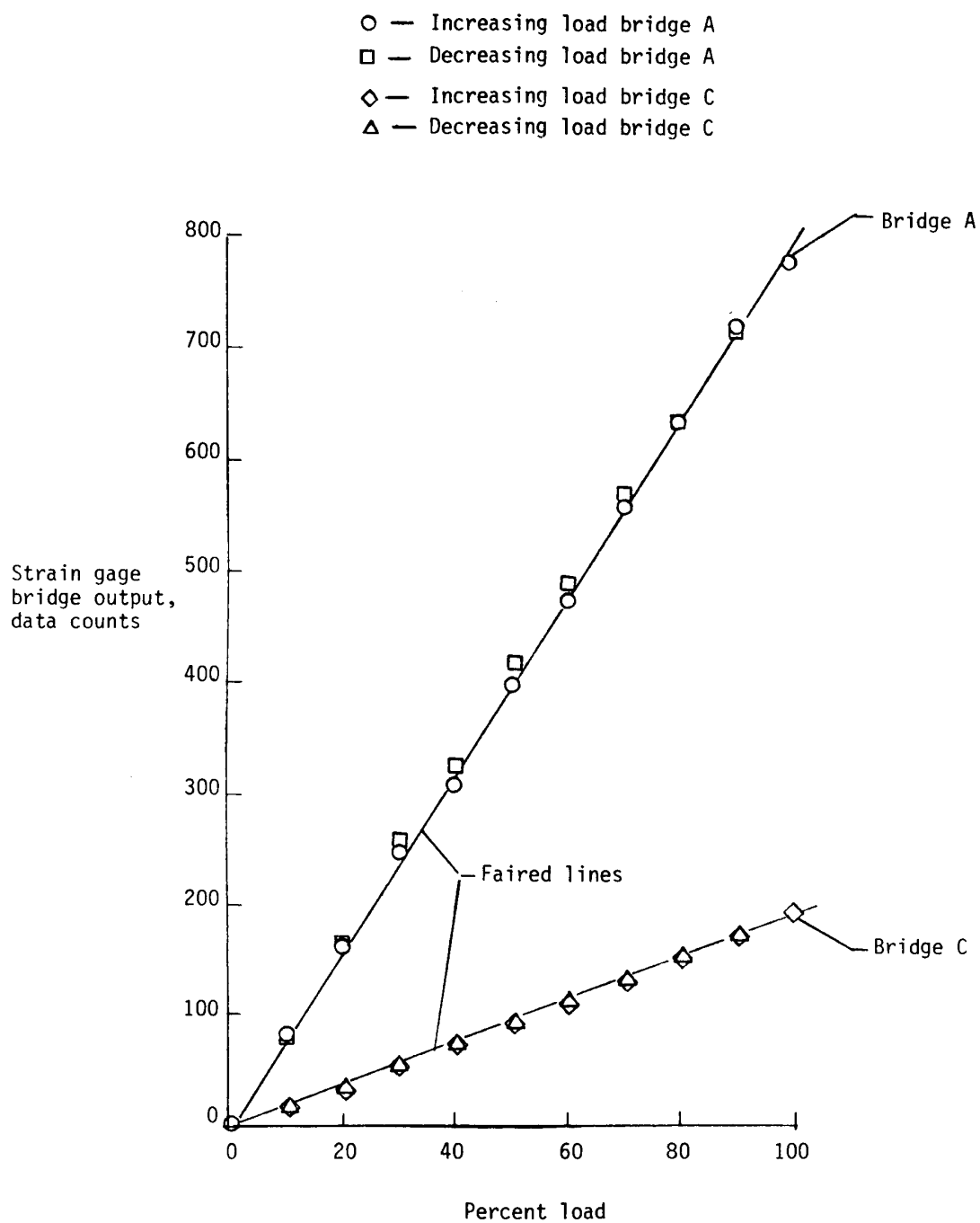


Figure 7. Typical strain gage bridge output as a function of the combined vertical and drag calibration load.

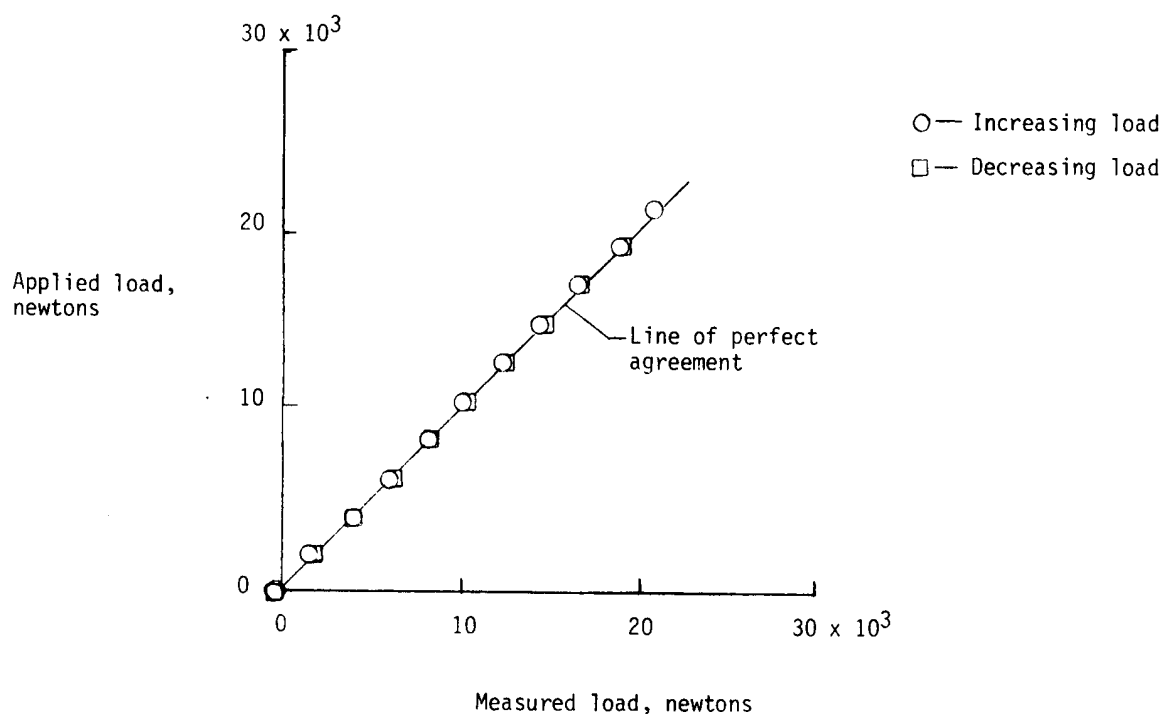


Figure 8. Applied versus measured drag load for the combined vertical and drag calibration load.

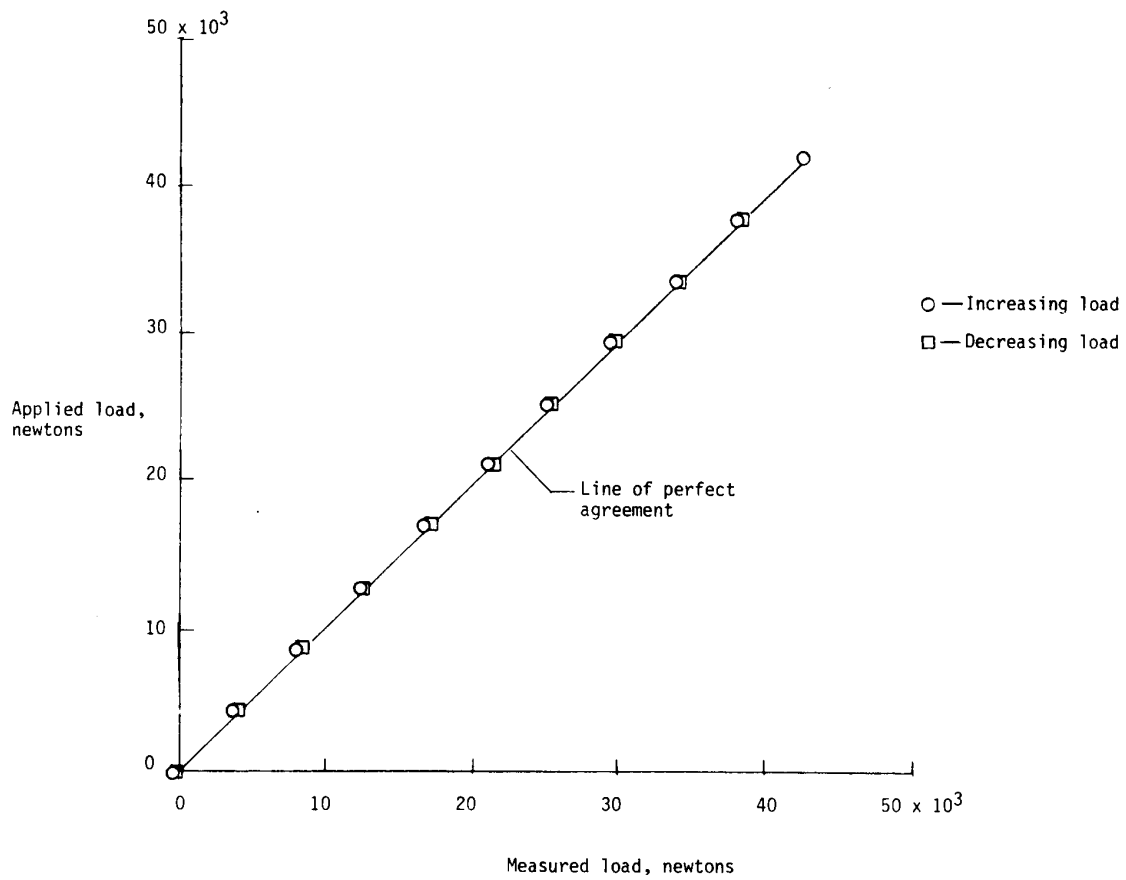


Figure 9. Applied versus measured vertical load for the combined vertical and drag calibration load.

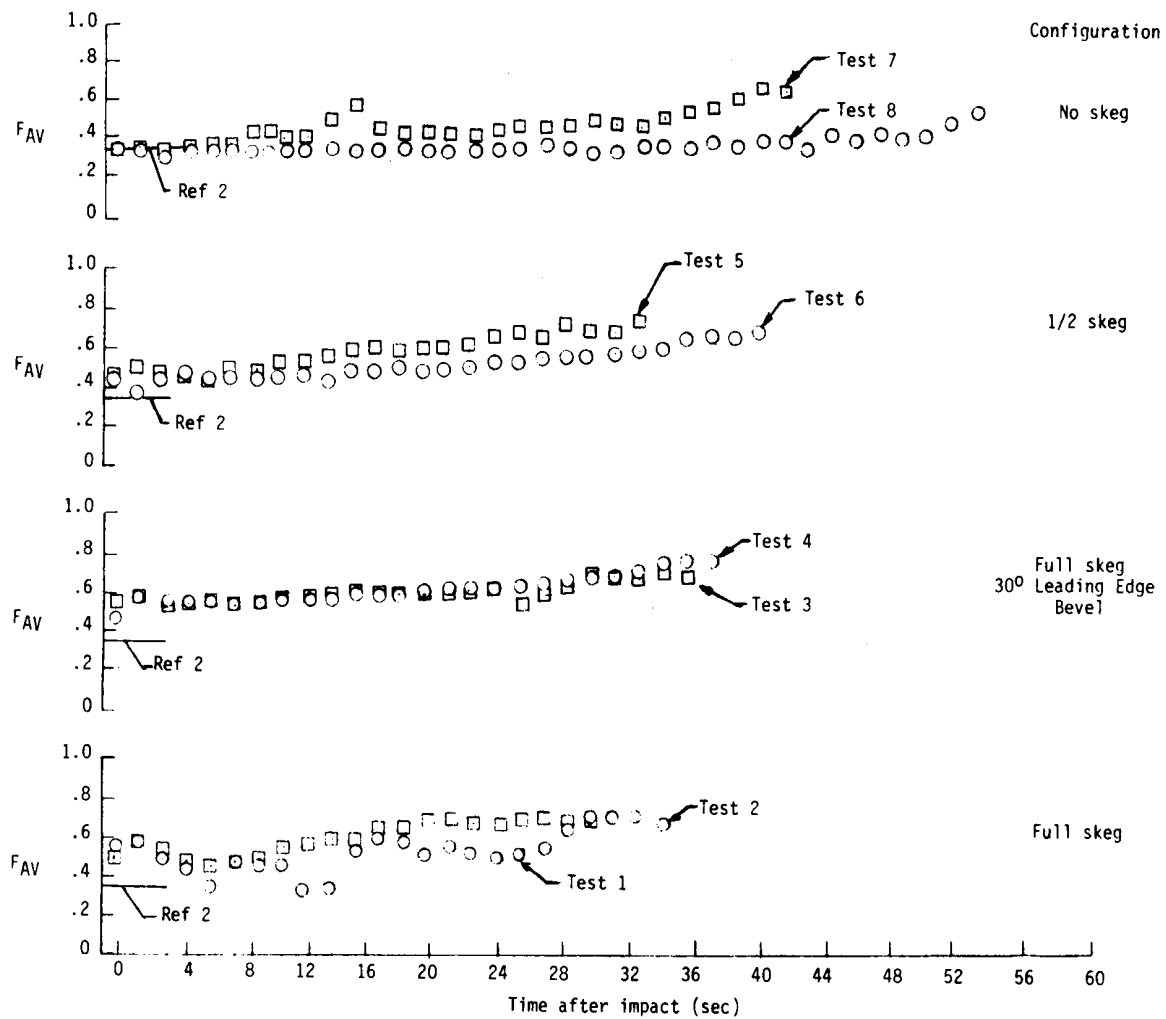


Figure 10. Time histories of average friction coefficient for test conditions 1 through 8.

